EurJIC

European Journal of Inorganic Chemistry

Chemistry Europe

European Chemical Societies Publishing

Accepted Article

Title: ZnO nanoparticles embedded on reduced graphene oxide nanosheet (ZnO-NPs@r-GO) as a proficient heterogeneous catalyst for one-pot A3-coupling reaction

Authors: Dikin Patel, Chetan K. Modi, Prafulla K. Jha, Himanshu Srivastava, and Sanjeev R. Kane

To be cited as: *Eur. J. Inorg. Chem.* 10.1002/ejic.202100368

Link to VoR: https://doi.org/10.1002/ejic.202100368

WILEY-VCH

10.1002/ejic.202100368

ZnO nanoparticles embedded on reduced graphene oxide nanosheet (ZnO-NPs@r-GO) as a proficient heterogeneous catalyst for one-pot A^3-coupling reaction

Dikin Patel[a], Chetan K. Modi[a]*, Prafulla K. Jha[b], Himanshu Srivastava[c], Mr. Sanjeev R. Kane[c]

[a] Dr. Dikin Patel, Dr. Chetan K. Modi
Applied Chemistry Department, Faculty of Technology & Engineering, The Maharaja Sayajirao University of Baroda, Vadodara-390 001, Gujarat, India
chetanmodi-appchem@msubaroda.ac.in
https://www.msubaroda.ac.in/Academics/Departments/teaching/

[b] Prof. Prafulla K. Jha
Department of Physics, Faculty of Science, The Maharaja Sayajirao University of Baroda, Vadodara, Gujarat 390 002, India

[c] Dr. Himanshu Srivastava, Mr. Sanjeev R. Kane
Synchrotrons Utilisation Section, Raja Ramanna Centre for Advanced Technology, Indore 452013, India

Abstract:

This study reports a simple and facile route for the synthesis of ZnO nanoparticles (ZnO-NPs) decorated on reduced graphene oxide nanosheet (ZnO-NPs@r-GO) as a heterogeneous catalyst and tested over multicomponent one-pot A^3-coupling reaction. The reduction of graphene oxide with the anchoring of ZnO-NPs on the r-GO nanosheet was observed through the X-ray diffraction patterns, Raman, FTIR, and XPS results of the ZnO-NPs@r-GO sample. ZnO-NPs (average particle size of 3.4±1.5 nm) with uniform size distribution over r-GO nanosheet were substantiated through HRTEM analysis. Impressively, ZnO-NPs@r-GO significantly used for A^3-coupling reaction with different aromatic aldehydes, active methylene compounds, and urea and under the optimized reaction conditions gave exceptional activity to produce synthetically valuable 3,4-dihydropyrimidinones products (possessing diverse therapeutic and pharmacological properties) i.e. 97% isolated yield of the product. In addition, excellent reusability up to 4 repeated cycles are the key advantages of the present catalyst used for this multicomponent A^3-coupling reaction.

Introduction

The nitrogen-based heterocyclic compounds have huge potential to be employed in wide range of applications such as their pharmaceutical,[1,2] biological activities,[3,4] magnetism,[5,6] luminescence,[7,8] catalysis[9,10] and so on. The formation of nitrogen-based heterocyclic compounds via A^3-coupling reaction involves the reaction between an aldehyde, β-keto ester, and urea or thio-urea is nowadays one of the most fascinated coupling reactions that used to produce dihydropyrimidinones (DHPMs). Additionally, these reactions are mild, low-cost and one-pot (in situ) synthesis. The product dihydropyrimidinones (DHPMs) has received a much attention owing to the discovery of the calcium channel modulating drug, Nifedipine, containing the DHPM backbone, was used for cardiovascular disease. The discovery of monastrol containing DHPMs compound was found effectual as an anticancer agent for inhibiting mitotic kinesin Eg5. Furthermore, DHPMs compounds viz. SQ 32547 and SWO_2 are found pertinent as a useful orally active antihypertensive agent. On the other hand, several esters and cyanide containing DHPMs are found suitable as antibacterial agents.[11-16]

In recent decades, the A^3- coupling reaction has been performed over strong acidic catalysts such as $TiCl_3$, $BF_3.OEt_2$, $ZrCl_4$, $InBr_3$, $BiCl_3$, Me_3SiCl, LiBr, $Mn(OAc)_3.2H_2O$, $La(OTf)_3$, $Yb(OTf)_3$, and $Sc(OTf)_3$. All of the aforesaid systems have been proposed to demonstrate more or less highly active and -selective products due to the presence of easily accessible active sites.[17-30] However, these systems are often regarded as imprecise with many impediments, including agglomeration of active sites; the contamination of toxic metal is also found along with the product which is comparatively detrimental one when dealing with the synthesis of biological products. In this regard, the non-recoverable catalyst from the product is the key challenging task in the research field. Therefore, to get rid out of these problems and minimize hazards in biological products, the solid supported catalysts have been widely preferred. In addition to this, the need for the solid supported catalysts is caused by the presence of large surface area, defects sites and excellent mechanical strength in relation to the total catalyst loading, which leads to easily adsorb of the more active site i.e. active metal precursor. At the present time, the effective and multifaceted solid supports such as silica, activated carbon, zeolites, SBA-15 and several others have been reported for one-pot coupling reaction including Homo coupling, cross-coupling and A^3-coupling reactions.[30-36] Previously, Fe_3O_4 nanoparticles embedded on the

mesoporous SBA-15 support using an "in situ" approach have been reported by D. Bhuyan and co-workers[37] and catalytically tested over A^3-coupling reaction. Bao-Dui Wang et al.[38] have been synthesized graphene-Fe_3O_4 catalyst with unwavering Fe_3O_4 NPs by the decomposition of $Fe(CO)_5$ on the surface of graphene oxide. The uniqueness of this work is that the decomposition products of $Fe(CO)_5$ retaliated with GO leading to the formation of graphene-Fe_3O_4. The resulting catalyst was tested over A^3-coupling reaction. Another work based on manganese-containing periodic mesoporous organo silica with ionic-liquid framework (Mn@PMO/IL) in the A^3-coupling reaction was investigated by D. Elhamifar and co-workers.[39]

Transition metal oxide shows enormous prospective in many important organic transformations due to their controlled shape, size, stability, a non toxic, crystallinity and functionality, corrosion resistance, easily scalable, relatively cost effective and non-hygroscopic property, making it as a proficient catalyst. In past few decades, rGO/ZnO nanocomposites have been explored in various fields such as electrochemical capacitors,[40] adsorbents for pollutants and removal of RhB dye from water,[41] photocatalysts and manufacture of organic photovoltaics.[31] Though for organic transformations,[43-44] ZnO nanoparticles (NPs) have been established as solitary heterogeneous catalysts however, to the best of our knowledge, only few reports on rGO/ZnO nanocomposites as catalysts have been reported in the literature.[45-47] In continuation of our earlier work[48-50], here in we report highly efficient ZnO-NPs@r-GO as a proficient heterogeneous catalyst and substantiated through various characterization tools. The accountability of rGO in ZnO-NPs@r-GO nanocatalyst is mainly providing tangible support which enhances the mechanical strength of the catalyst and also uniform dispersibility of ZnO-NPs. In addition to this, the active sites are easily accessible to the substrate molecule to be adsorbed effortlessly, which aids in easy recoverability and recyclability of the catalyst.[51,52] The catalytic aptitude in terms of superiority, consistency and vitality was inspected over one-pot A^3-coupling reaction with different aromatic aldehydes, active methylene compounds and urea. The impact of discrete parameters influencing catalytic activity such as catalyst dosage, solvent, varying amount of urea and time has also been monitored.

Results and discussion

The aforesaid synthesized ZnO-NPs@r-GO nanocatalyst was thoroughly corroborated by various physico-chemical techniques such as FT-IR, Raman, XRD, XPS, HR-TEM, and thermogravimetric analysis. The results of as-prepared nanocatalysts have been discussed as follows:

In view of the fact that the Raman spectroscopy is an imperative tool to construe the structure in predominantly defects and disorder nature of graphene-based materials. The Raman spectrum of ZnO-NPs@r-GO nanocatalyst is shown in Fig. 1, which exhibits two notable peaks at around ~1383 and ~1563 cm^{-1} subsequent to the precise D- and G- band, respectively.

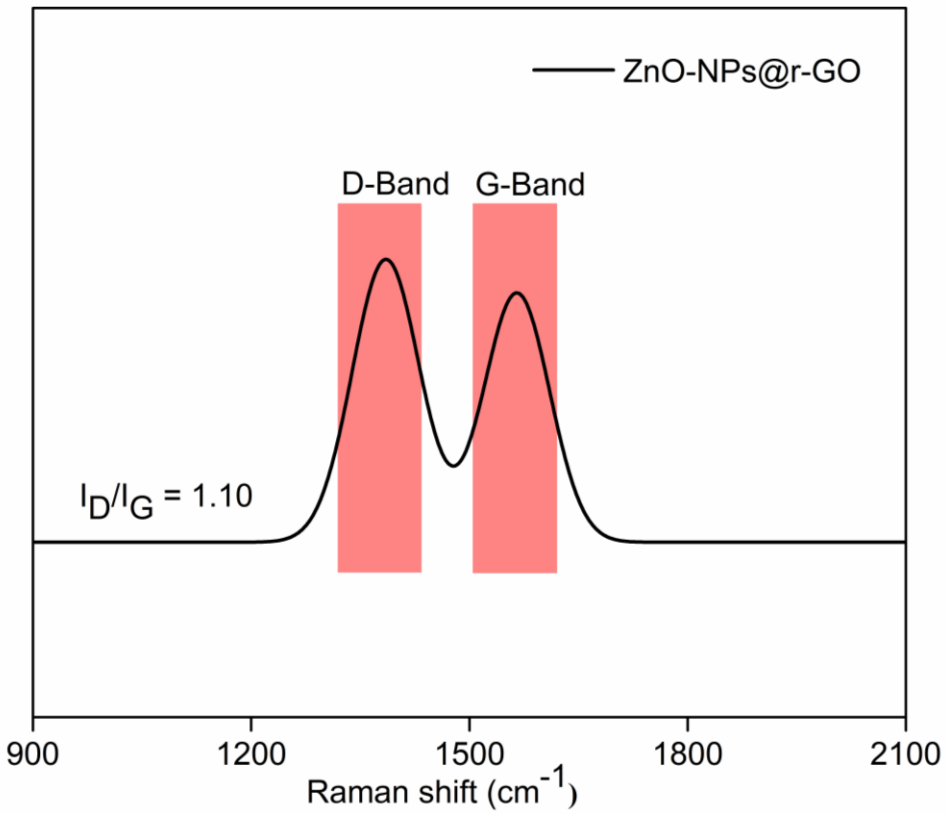

Figure 1. The Raman spectrum of ZnO-NPs@r-GO.

The graphitic peak (G band) at ~1563 cm^{-1} is owing to the E_{2g} vibrational mode of the C-C bond stretching, arises due to the sp^2 carbon network of the graphene plane, whereas, the disorder peak (D band) at ~1383 cm^{-1} is due to symmetry forbidden band of the longitudinal plane phonon vibration or k-point phonons of the A_{1g} vibrational mode.[53] The intensity ratio of the D and G

bands i.e. (I_D/I_G ratio) facilitates to estimate the defects of graphene based compounds where a higher ratio makes sure of more defects on graphene. The calculated I_D/I_G ratio of ZnO-NPs@r-GO nanocatalyst is 1.10, which is comparable to the spectrum of GO (fig. S1).The increment in the intensity ratio was might be due to the attachment of the metal ion on the surface of GO. Furthermore, we have also calculated the crystalline size of ZnO-NPs@r-GO nanocatalyst (i. e. La = 17.48 nm) using Tuinstra–Koenig relation.[54]

The XRD patterns are the prominent technique used to determine the crystallinity of as-prepared nanocatalysts. The XRD patterns of ZnO-NPs and ZnO-NPs@r-GO nanocatalysts are shown in Fig. 2 whereas, XRD patterns of GO is given in supplementary file (see Fig. S2). The peak observed at 11.8^o in the XRD pattern of GO, which has been disappeared and a new diffraction peak is observed at 24.3^o (Fig. 2) with inter-layered distance of 3.6 Å after the *in situ* anchoring of ZnO nanoparticles and reduction of GO nanosheets. This result clearly indicates that some of the oxygen containing debris have been abolished and the formation of new in-plane sp^2 domains during the reduction process. The aforesaid results are in well accordance with Raman and XPS results.

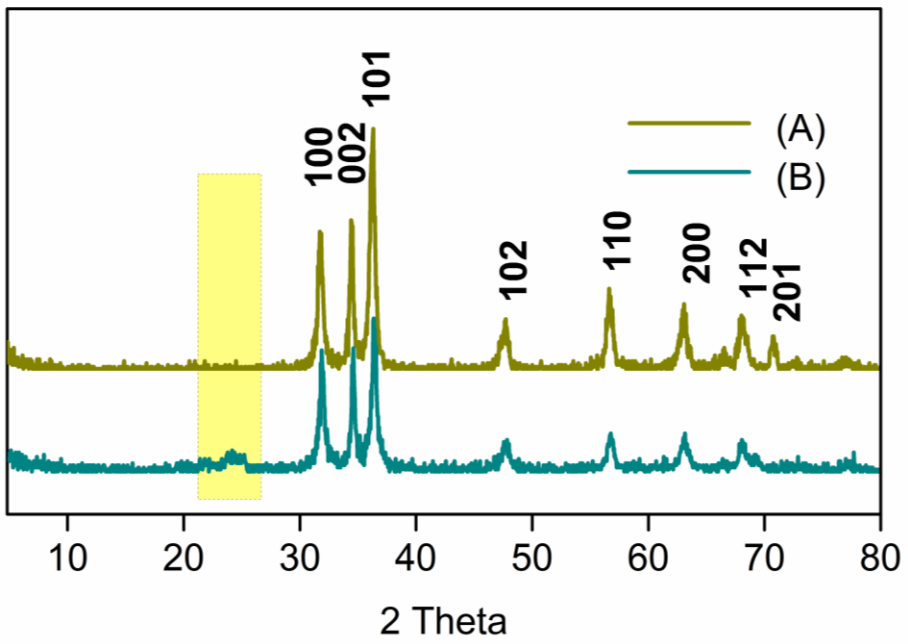

Figure 2. XRD patterns of (A) ZnO-NPs and (B) ZnO-NPs@r-GO.

In the XRD patterns of ZnO-NPs@r-GO nanocatalyst [Fig. 2(B)], the diffraction peaks at 31.7º, 34.4º, 36.1º, 47.6º, 56.7º, 62.9º, 68.0º and 70.9º were reconcilable with those of (1 0 0), (0 0 2), (1 0 1), (1 0 2), (1 1 0), (1 0 3), and (1 1 2), respectively,[55] pointing towards the hexagonal wurtzite structure of ZnO (JPCDS 36-1451). These results are more uniform to that observed in neat ZnO-NPs XRD patterns [Fig. 2(A)].[56] The diffraction peak observed at 24.3º, due to the distinctive absorption peak for graphene. Whereas no such peak was observed together with no strong absorption observed at the diffraction peak of 11.8º, suggesting that the GO is changed into reduced graphene oxide during the reduction process.

The surface chemical composition and bonding environment of as-prepared nanocatalyst was analyzed by the X-ray photoelectron spectroscopy (XPS). As shown in Fig. 3(A), the survey spectra of ZnO-NPs@r-GO are displayed three prominent elements C 1S, O 1S and Zn 2p at about 282.9, 534.8, and 1031.8, respectively. In the Zn 2p core level spectra [Fig. 3(B)], two prominent peaks observed at 1022.6 eV and 1045.6 eV corresponds to Zn $2p_{3/2}$ and Zn $2p_{1/2}$, respectively, indicating that Zn was present in the form of zinc oxide.

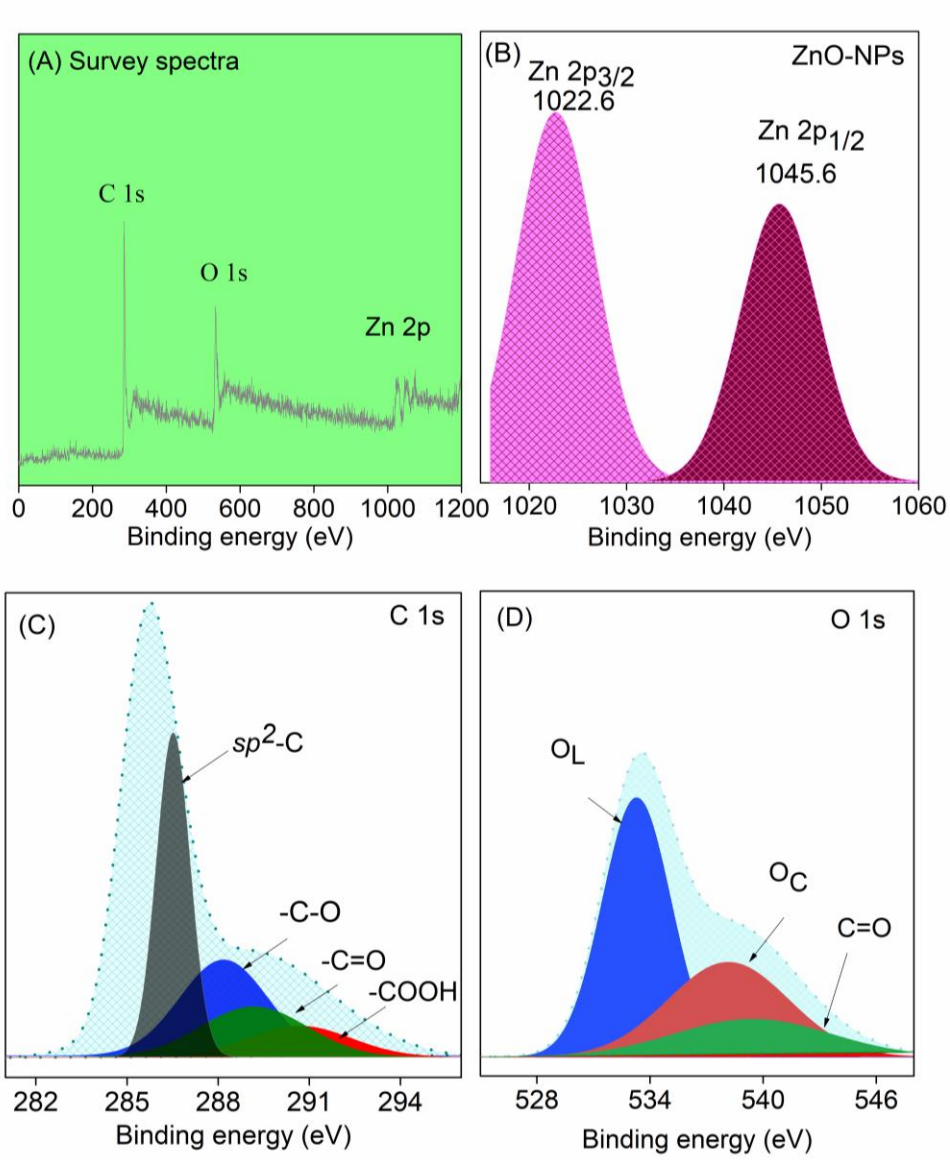

Figure 3. XPS spectra (A) survey spectra of ZnO-NPs@r-GO, (B) Zn sp core level spectrum, (C) C 1s spectra of ZnO-NPs@r-GO and (D) O 1s spectra of ZnO-NPs@r-GO.

While comparing C 1s spectra of GO (Fig. S3) with the high-resolution C 1s spectra of ZnO-NPs@r-GO nanocatalyst [Fig. 3(C)] four prominent peaks observed at 286.4, 288.2, 289.3 and 291.3 eV, assigned to sp^2-C, -C–O, -C=O, and -COOH, respectively. These results showed that the intensity of peaks -C–O, -C=O and-COOH was considerably low and while the magnitude of sp^2-C peak was dramatically increased owing to the restoration of the sp^2 domains in the new plane. These results are in well agreement with the Raman spectra. The high resolution O 1s spectrum of ZnO-NPs@r-GO nanocatalyst [Fig. 3(D)] has shown three peaks at ~533.2, ~538.2

and ~539.3 eV. Among them, the first two peaks are attributed to the lattice oxygen (O_L) and chemisorbed oxygen (O_C) species, respectively, whereas the later peak observed at ~539.3 eV, indicating the C=O bond in the wurtzite structure of hexagonal ZnO. In addition, we have calculated loading amount of ZnO using quantitative XPS and observed of about 0.6% loading in ZnONPs@rGO catalyst.

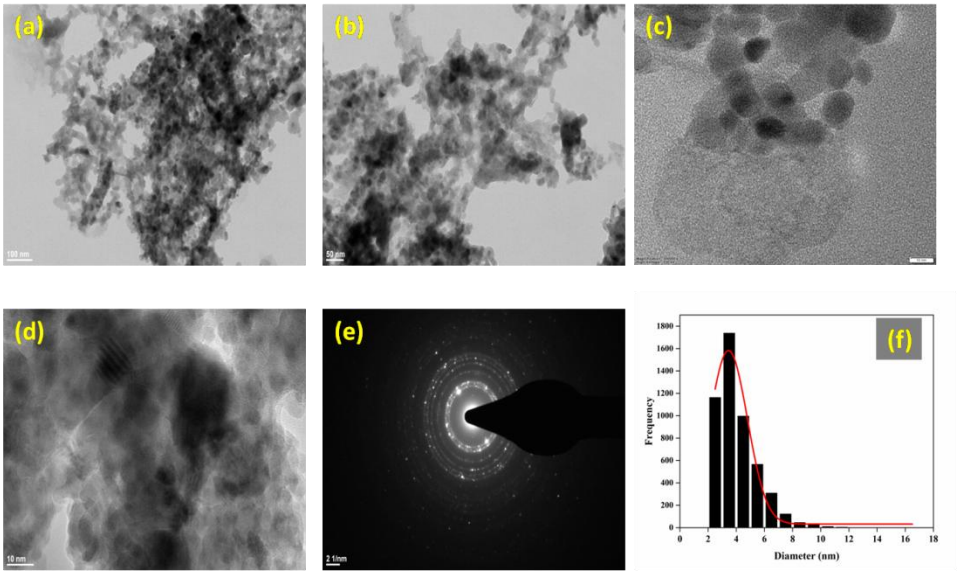

Figure 4. (a, b) Low magnification TEM image of ZnO-NPs@r-GO, (c, d) HR-TEM image of ZnO-NPs@r-GO with fringe spacing, (e) SAED pattern of ZnO-NPs@r-GO, (f) Histogram graph of ZnO-NPs@r-GO.

The HR-TEM images of ZnO-NPs@r-GO nanocatalyst are shown in Fig. 4. The TEM images of ZnO-NPs@r-GO demonstrated the fine narrow sized ZnO nanoparticles were dispersed on rGO nanosheet [Fig. 4 (a, b)].The ZnO nanoparticles have observed an average particle size of 3.4±1.5 nm [Fig. 4(f)]and have clearly shown the size distribution of ZnO nanoparticles on the rGO nanosheet, which was investigated by ImageJ software. As depicted in Fig. 4(d), the nanocatalyst has given the information pertaining to the crystal lattice fringes of ZnO-NPs with a d-spacing of 0.22 nm, indicating with the plane of cubic ZnO-NPs. In the SAED image of ZnO-NPs@r-GO [Fig. 4(e)], the diffraction pattern was perceived, which substantiates the polycrystalline nature of ZnO-NPs on the surface of r-GO nanosheets. The intense spherical dots

of ZnO-NPs were also observed in the SAED pattern. These results are in well agreement with the XRD data as discussed above.

The FTIR spectra of ZnO-NPs and ZnO-NPs@r-GO are shown in Fig. 5. In the FTIR spectrum of ZnO-NPs, the band observed at 496 cm^{-1}, which indicates the vibrational mode of Zn-O bonds. However, in the spectrum of ZnO-NPs@r-GO, this band was slightly moved towards the lower wavelength (480 cm^{-1}), which might be due to ZnO nanoparticle supported on rGO nanosheet.[57]

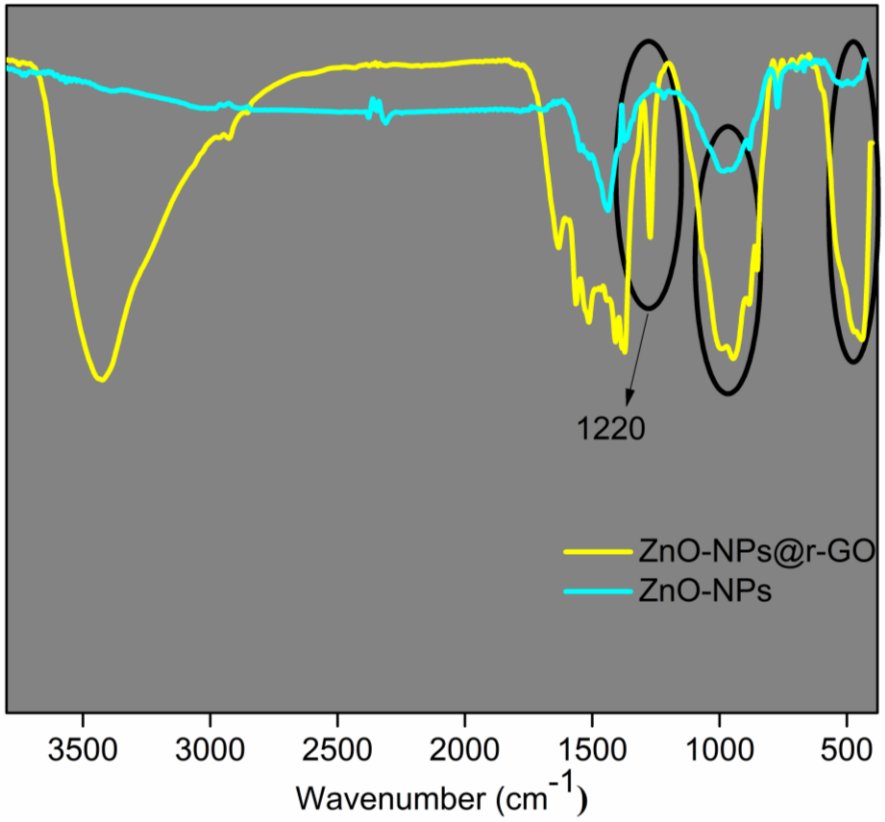

Figure 5. FTIR spectra of ZnO-NPs and ZnO-NPs@r-GO.

Moreover, the peak observed in the FTIR spectrum of ZnO-NPs at ~950 cm^{-1} is assigned to Zn-OH bonds. The same band was also seen in the FTIR spectrum of ZnO-NPs@r-GO. In the FTIR spectrum of ZnO-NPs@r-GO, two additional stretching vibrations are observed at ~3440 and in the region, 2860-2880 cm^{-1}, are corresponding to the -OH and aromatic C-H stretching vibrations, respectively. In the FTIR spectra of GO (Fig. S5), the intense peak observed at

around 1700 cm^{-1} is due to $\upsilon_{(C=O)}$ stretching vibration of the –COOH group, was disappeared in the spectra of ZnO-NPs@r-GO. In addition to this, one prominent peak observed at 1220 cm^{-1} in the spectra of ZnO-NPs@r-GO, is due to the epoxy group and was remained intact after the chemical reduction process.[58]

In the subsequent section, the thermal behavior of the as-synthesized catalyst, characterized on the basis of thermogravimetric method is discussed. The quantitative purpose of the organic content and the thermal stability of the compound have been achieved through the thermogravimetric analysis. The thermogram of ZnO-NPs@r-GO nanocatalyst is fairly matched with GO. As shown in Fig. 6, the first weight loss (~6.2%) observed in the temperature range 110-280 ºC is assigned to the removal of the most of the oxygen containing functional groups. This was followed by a gradual plunge in the weight loss of 49.6% in the temperature range of 400- 650 ºC, assumed to be due to the pyrolysis of carbonaceous stuff of the graphene nanosheets.

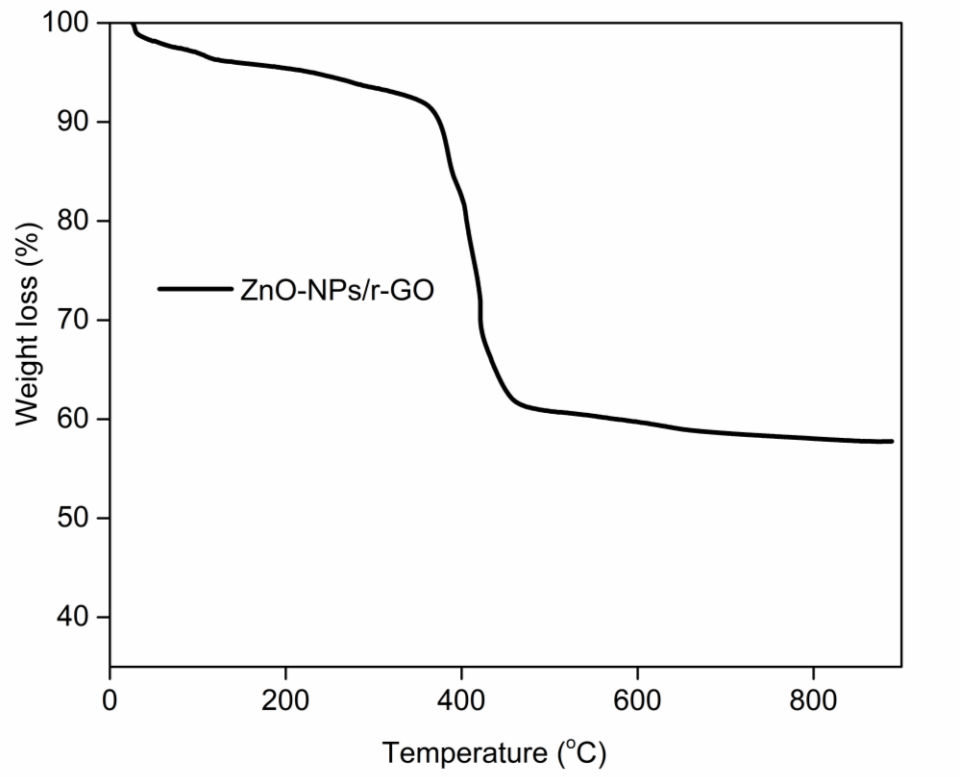

Figure 6. TG analysis of ZnO-NPs@r-GO.

Catalytic study

In the previous section, as-prepared nanocatalysts have been successfully synthesized and characterized. However, herein this segment, we have discussed the catalytic activity of as-synthesized nanocatalysts executed over the One-pot A^3-coupling reaction using aldehyde, ethyl acetoacetate and urea as starting materials and ethanol as a greener solvent to form 3,4-dihydropyrimidin-2 (1H)-ones as the main product (Scheme 1).

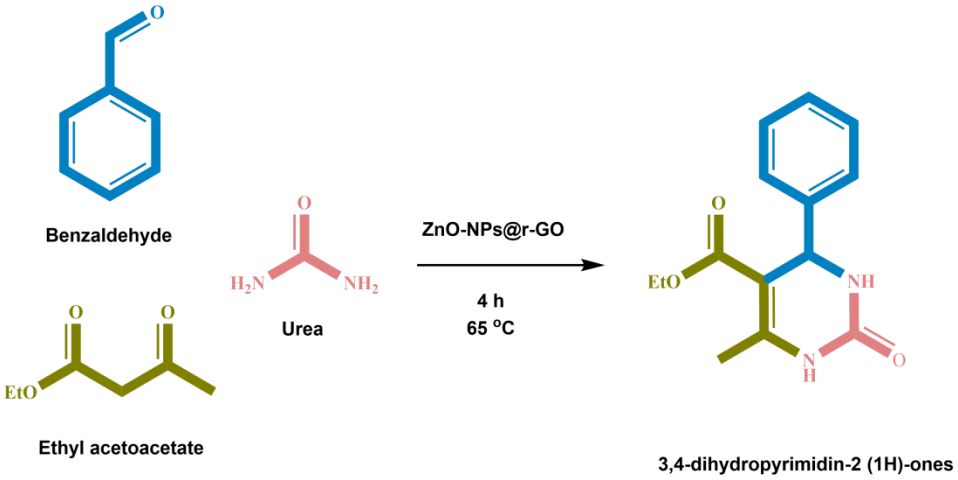

Scheme 1. A schematic representation of Biginelli reaction.

Under the typical reaction conditions, A^3-components i.e. Benzaldehyde (1 mmol), ethyl acetate (1 mmol) and urea (0.8 mmol) were dissolved into 5 mL ethanol and then 10 mg catalyst was taken in RBF. To acquire the optimum results, first, all the catalysts like GO, ZnO, CuO, $Zn(CH_3COO)_2$, $Cu(NO_3)_2$, ZnO-NPs@r-GO, and Cu-NPs@r-GO were employed to get best-suited catalyst for this Biginelli reaction and the results are shown in Fig. 7. The results clearly indicate lower yields are observed with species like GO, ZnO, CuO, $Zn(CH_3COO)_2$, $Cu(NO_3)_2$ and without catalyst. However, the conspicuous results are observed with supported systems like ZnO-NPs@r-GO and Cu-NPs@r-GO. Amongst them, ZnO-NPs@r-GO has found most suitable catalyst giving optimal yield (84%) under the optimized conditions and therefore, it has been chosen for further experiments.

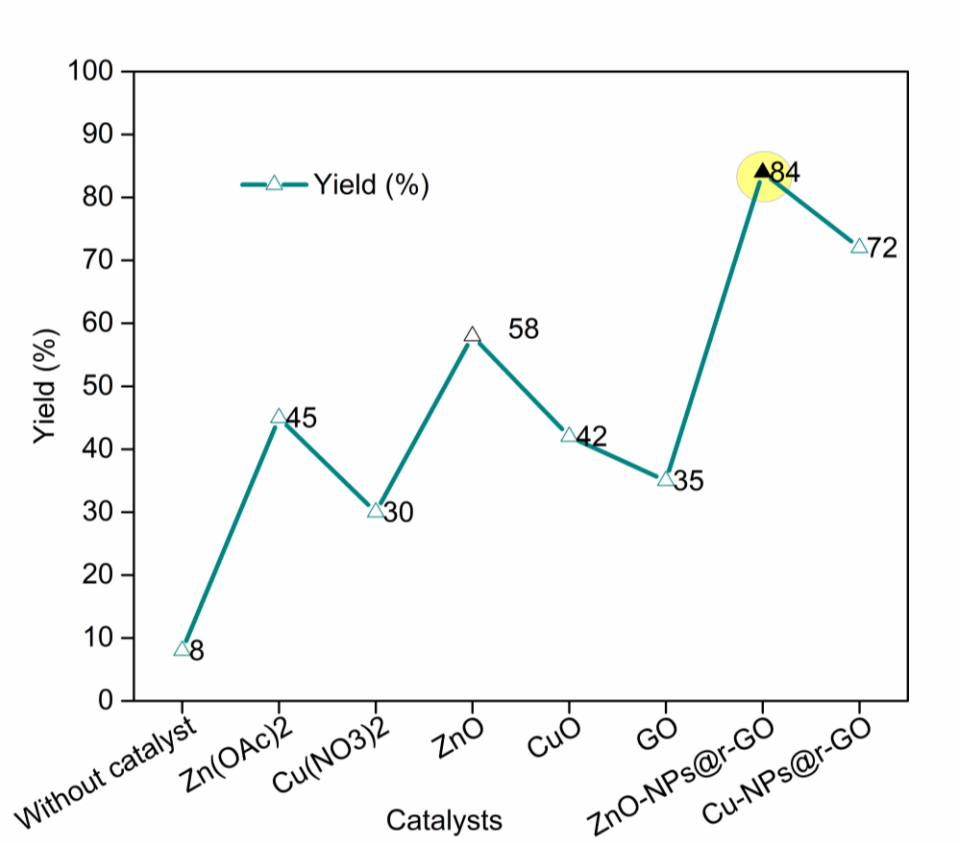

Figure 7. The catalytic activity of various catalysts for one-pot A^3-coupling reaction. Reaction conditions: benzaldehyde (1 mmol), Ethyl acetoacetate (1 mmol), Urea (1.2 mmol) varying catalysts (10 mg), Ethanol (5 mL), temp. (Reflux i.e. 75 ºC), Time (3.5 h).

Factor affecting the one-pot A^3-coupling reactions

Effect of catalyst dosage

The catalyst concentration is a one of the significant aspects in the A^3-coupling reaction. As shown in Fig. 8, five different dosages viz. 5 mg, 10 mg, 15 mg, 20 mg, and 30 mg of the representative catalyst, i.e. ZnO-NPs@r-GO were taken with keeping all other reaction parameters fixed: temperature (65°C), benzaldehyde (1 mmol), ethyl acetoacetate (1 mmol), urea (1.2 mmol), ethanol (5 mL), and reaction time (3.5 h).The results are shown in Fig. 8. The maximum yield (93%) of the product was achieved with 15 mg of catalyst. While further increasing the catalyst amount showed a downward trend of the product yield (see Fig. 8). The reduction trend in the product yield was might be due to certain concentration of the product

adsorbed on the catalytic active sites. As a result, the optimal catalyst amount has taken to be 15 mg for the further investigation.

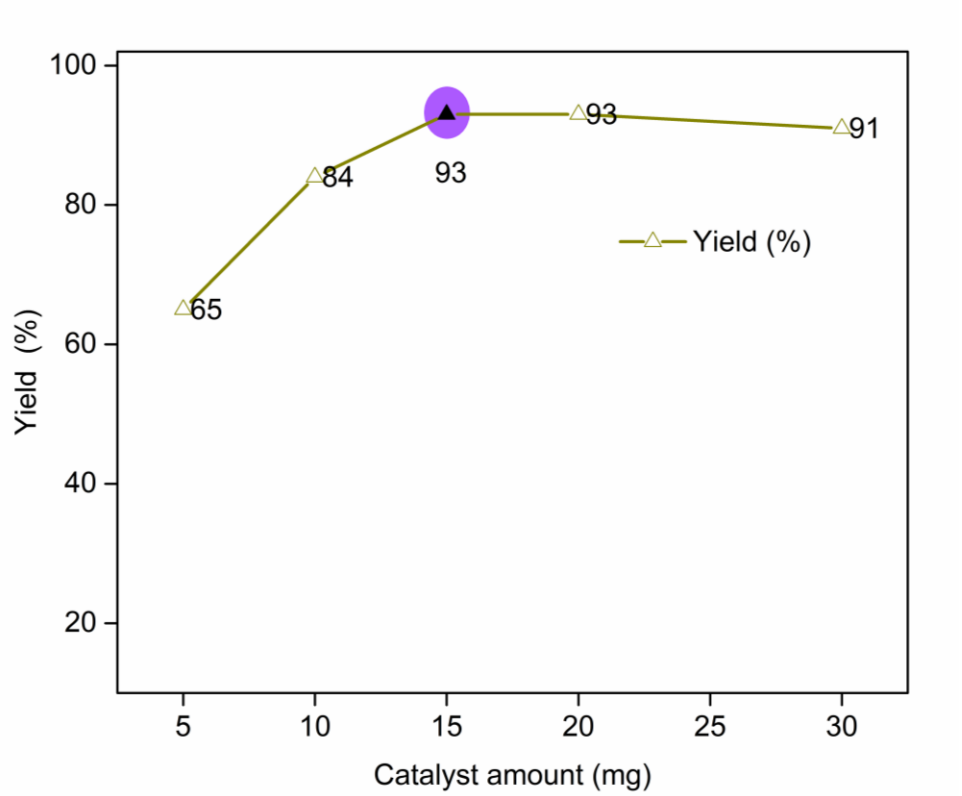

Figure 8. The effect of catalyst dosage for One-pot A^3-coupling reaction.
Reaction conditions: benzaldehyde (1 mmol), Ethyl acetoacetate (1 mmol), Urea (1.2 mmol) ZnO-NPs@r-GO (**X** mg), Ethanol (5 mL), temp. (Reflux), Time (3.5 h).

Effect of various solvents

The effect of varying solvents such as polar protic i.e. ethanol, polar aprotic i.e. acetonitrile (ACN) and non-polar i.e. toluene was examined (Fig. S7) over A^3-coupling reaction with other parameters kept fixed to increase the yield of the product. As shown in Fig. S7, the product yield achieved with different solvent systems in the decreasing order as Ethanol (93%) > ACN (75%) > toluene (51%). Initially, we have also performed the aforesaid catalytic reaction without solvent, however; as prophecy, we could not observe the as-expected elevated yield (21%). Among the various solvent systems, when ethanol was utilized, an optimum yield of the product (93%) was obtained. Consequently, ethanol is preferred to be used as a solvent for the aforesaid reaction.

Effect of amount of urea

Varying amounts of urea such as 1:1:0.8, 1:1:1, 1:1:1.2, and 1:1:1.4 with benzaldehyde, ethyl acetoacetate are employed to examine their effect on the A^3- coupling reaction with keeping all other parameters fixed. A key role of urea is clearly perceptible from Fig. S8. Highest product yield of 3,4-dihydropyrimidin-2 (1H)-ones (97%) is obtained with 1:1:1 mole ratio, while on further increasing the concentration of urea with increasing mole ratios i.e. 1:1:1.2 and 1:1:1.4,a downtrend is observed with product yield of 93% and 89%, respectively. This reduction was believed to be due to the probability of the extra urea and water to form ammonium. Hence, 1:1:1 mole ratio is preferred for the further experiments keeping other parameters fixed.

Effect of Time

To obtain the precise isolated yield of the product, it is of rather imperative to end up the reaction at accurate time. This study is aiming to find out the accurate time for this multicomponent A^3-coupling reaction using ZnO-NPs@r-GO as a representative catalyst. As shown in Fig. S9, we have conducted this experiment at five different time viz. 1, 2, 3, 3.5 and 5 h by keeping other parameters fixed. It can be seen from the figure that to begin with at 1 h, 42% isolated product yield was attained. However, on enduring the reaction with time, the product yield also upholds in the increasing trend and achieved maximum (97%) at 3.5 h. If the reaction still continued to 5 h, no further increment in the yield of the product was achieved. As a result, we have chosen 3.5 h as the ideal time for further examination of other experimental variables.

After getting the optimized conditions, we have further been exploring the scope of A^3-coupling reaction etiquette by altering substrates like aldehydes, ethyl and/or methyl acetoacetate and urea producing a wide range of dihydropyrimidinones (DHPMs) and its derivatives (Table 1). While the reactions using various aldehydes including 4-methyl benzaldehyde and/or 4-methoxy benzaldehyde, furfuraldehyde and ethyl acetoacetate and urea gave comparatively exceptional yield than the product yields acquired using various aldehydes, methyl acetoacetate and urea (Table 1). Consequently, ethyl acetoacetate is quite better substrate than methyl acetoacetate.[59]

Table 1. The scope of ZnO-NPs@r-GO nanocatalyst over Biginelli condensation reaction using various aldehydes, β-keto esters and urea

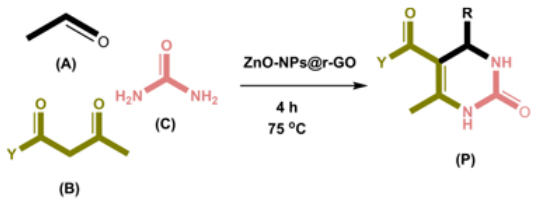

Entry	(A)	(B)	(C)	Yield (%)	Melting point (°C)	[a]TON
1				97	203-205	27.0
				90	213-214	26.2
2				89	196-198	23.3
				82	201-202	22.9
3	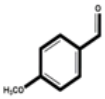			88	201-203	21.8
				83	190-193	21.8
4				90	206-208	25.5
				87	202-203	26.2

[a]TON (turnover number) = Moles of desired product formed/moles of catalyst.

A plausible mechanism for the Biginelli condensation reaction using ZnO-NPs@r-GO as a representative catalyst is demonstrated in Scheme 2. The reaction begins with the activation of a carbonyl group via the attachment of the substrate (aromatic aldehyde) onto the active site of ZnO-NPs@r-GO, followed by the nucleophilic attack of urea to an activated aldehyde, so as to generate the intermediate species (i.e. imine adduct). This imine intermediate is attacked by an ethyl acetoacetate molecule forming another intermediate (Scheme 2). It was then followed by the addition-elimination reactions, leading to the formation of the desired product.[59]

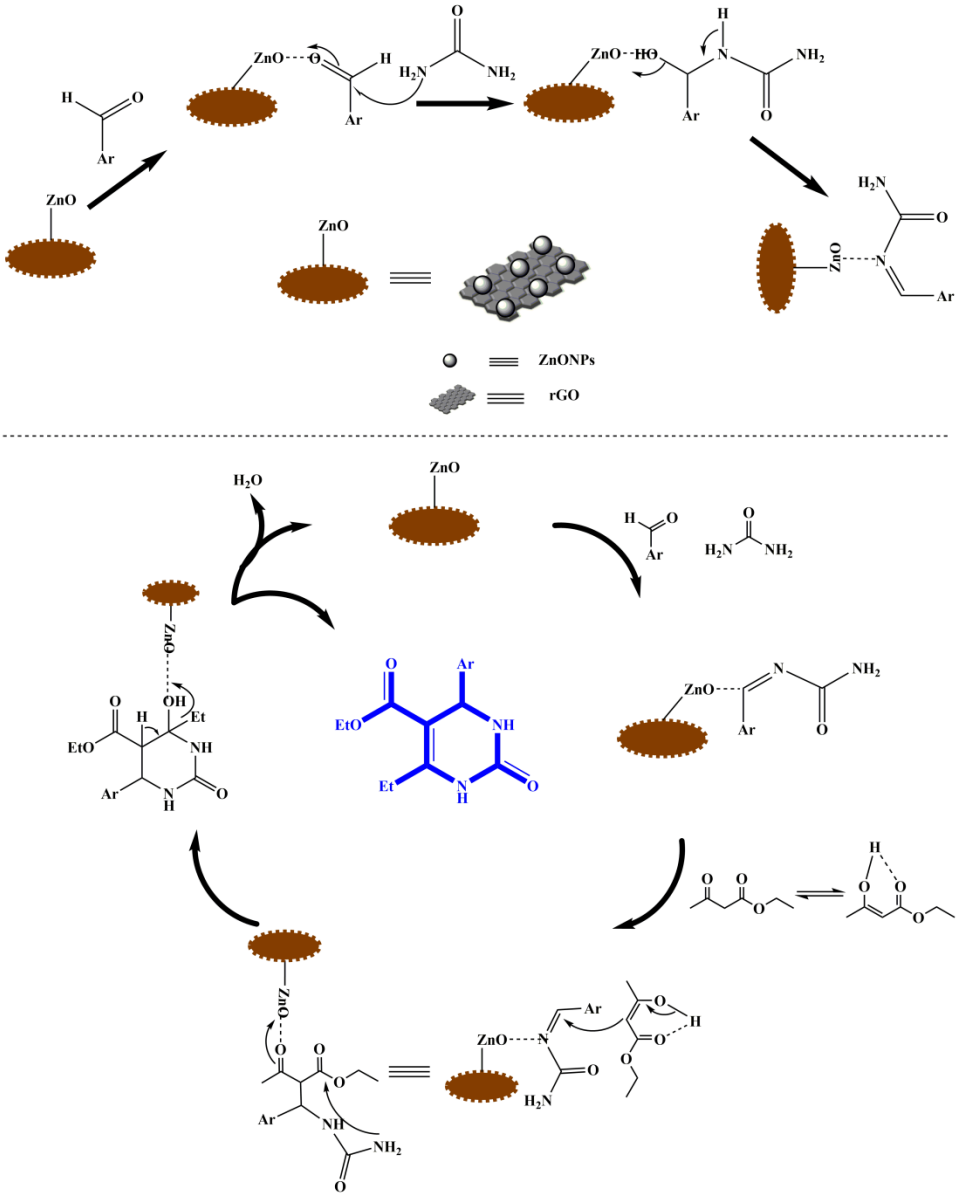

Scheme 2. A plausible reaction mechanism for the Biginelli condensation reaction over ZnO-NPs@r-GO nanocatalyst.

Recyclability

The reusability of the catalyst is of enormous consequence applicable to any heterogeneous catalytic system. The reusability of ZnO-NPs@r-GO as a representative catalyst was tested over A^3-coupling reaction and the results are shown in Fig. S10. Prior to examine this, the catalyst is recovered from the reaction mixture by filtration and washed several times with acetonitrile

followed by drying in an oven before utilizing for the further catalytic test. As seen in Fig. S10 it was recycled up to 5 times without any significant loss in activity, despite the fact that in the 4th and 5th run, the product yield decreasing up to 93% and 90%, respectively.[59]

Table 2. Comparative study

No.	Catalysts	Conditions	Time	Yield (%)	Ref.
1	Fe_3O_4@SBA-15 (0.084)	EtOH, 363 K	6 h	85	60
2	D-Xylonic acid	100, D-Xylonic acid	5 h	89	61
3	Partially Fluorinated, Water-Stable Cu(II)−MOF	60, Solvent free	2 h	89	62
4	PPF-SO_3H(sulfonic acid functionalized polypropylene fiber)	Reflux, Ethanol	8 h	74	63
5	12-Tungstophosphoric acid	Reflux, AcOH	6-7 h	70	64
6	$FeCl_3 6H_20$	Relux, CAN	12 h	88	65
7	Green-CuO NPs	90 °C, Ethanol	50 min.	98	66
8	ZnO-NPs@r-GO	75 °C, EtOH	3.5 h	97	Present work

In the past couple of years, catalytic studies over A^3-coupling reaction by various research groups using diverse homogeneous and/or heterogeneous catalysts have been discussed and are tabulated in Table 2. J. Mondal et al.[60] have executed the Biginelli reaction over Fe_3O_4@SBA-15 as an efficient heterogeneous catalyst using ethanol as a solvent at 90 ^oC, achieving 85% product yield after 6 h (Table 2, entry 1). J. Ma et al.[61] have accomplished Biginelli reaction over D-Xylonic acid as a catalyst, getting 89% product yield after 5 h at 100 ^oC (Table 2 entry 2). T. K. Pal et al.[62] developed a partially fluorinated, water-stable Cu(II)−MOF catalytic system, achieving a maximum of 89% product yield at 60 ^oC after 2 h (Table 2, entry 3). Shi and co-workers[63] have reported the Biginelli reaction catalyzed by PPF-SO_3H (sulfonic acid functionalized polypropylene fiber) using ethanol as a solvent under reflux for 8 h, achieving 74% product yield (Table 2, entry 4). Heravi and co-workers[64] have used 12-Tungstophosphoric acid as a catalyst for Biginelli reaction under reflux for 6-7 h, achieving 70% of the product yield

(Table 2, entry 5). Furthermore, $FeCl_3 \cdot 6H_2O$ used as a catalyst by ZT Wang and co-workers[65] over Biginelli reaction using acetonitrile as a solvent (under 12 h reflux time), obtaining 88% of the product yield (Table 2, entry 6). Sujahta et al[66] have used green CuO nanoparticles as catalyst for Biginelli reaction under 90 ^{o}C for 50 min, obtaining 98% of the product yield (Table 2, entry 7). Here in this work, our own results (Table 2, entry 8) show that, when ZnO-NPs@r-GO was used for 'one-pot' A^3-coupling reaction under optimized reaction condition bestowed exceptional product yield of 97% in 3.5 h under refluxing temperature i.e. 75 ºC.

Conclusion

In concluding remarks, we have synthesized highly efficient ZnO-NPs@r-GO as a proficient heterogeneous catalyst for one-pot A^3-coupling reaction. Graphene oxide was synthesized using modified Hummer's method and during the anchoring of ZnO-NPs on rGO nanosheet; graphene oxide was subjected to partial reduction as observed from the X-ray diffraction patterns, Raman, FTIR and XPS results of ZnO-NPs@r-GO sample. ZnO-NPs were found to be successfully diffused over the surface of rGO nanosheet as substantiated from HRTEM analysis with average particle size of 3.4±1.5 nm was investigated by ImageJ software. The intense spherical dots of ZnO-NPs were also examined in the SAED pattern. The as-synthesized ZnO-NPs@r-GO catalyst demonstrated exceptional catalytic activity for one-pot A^3-coupling (Biginelli condensation) reaction under the optimized reaction conditions to give preferred DHPM products in good to admirable yields. Besides, the plausible catalytic mechanism for the aforesaid condensation reaction has also been proposed and discussed. The nanocatalyst ZnO-NPs@r-GO also exhibited remarkable stability, recyclability and leaching-resistant performance with recycled up to four times without significant loss of activity.

Experimental Section

Materials

Natural flake graphite (325 mesh, 99.95%) was purchased from Sigma Aldrich. potassium permanganate, zinc acetate was acquired from MERCK India Pvt Ltd. Urea, ethyl acetoacetate, methyl acetoacetate, sulphuric acid, sodium nitrate, l-ascorbic acid, hydrochloric acid, 30% hydrogen peroxide, benzaldehyde, 4-methyl benzaldehyde, 4-methoxy benzaldehyde,

furfuraldehyde, 4-nitro benzaldehyde were procured from S D Fine Chem Ltd. All the materials are of analytical grade and used as received without further purification.

Synthesis of graphene oxide (GO)

Graphene oxide was synthesized from graphite flakes using a modified Hummer's method.[49, 67]

Synthesis of ZnO nanoparticles (ZnO-NPs)

The ZnO-NPs were prepared as follows: Zinc acetate dehydrate (2 g) was dissolved in 20 mL of deionized water. This aqueous solution of zinc acetate was then heated at 70 ºC with continuous stirring in a magnetic stirrer. Then, a freshly prepared (4 g) NaOH solution was added drop wise into an aqueous solution of zinc acetate with constant stirring and refluxed for 4 h at 70 ºC. The obtained white suspension was filtered, carefully washed with deionized water (until the pH maintained up to 6), dried in air oven at 70 °C and finally calcined at 550 °C for 6 h to get white powder of ZnO-NPs.

$$Zn(CH_3COO)_2 + NaOH \longrightarrow Zn(OH)_2 + 2CH_3COONa;$$

$$Zn(OH)_2 \longrightarrow ZnO + H_2O$$

Synthesis of ZnO-NPs@r-GO nanocatalyst

A 50 mg of GO was dispersed into deionized water (15 mL) in a 250 mL beaker followed by a dropwise addition of 10 mmol $Zn(CH_3COO)_2$ solution and then ultrasonicated for 20 min to produce uniformly dispersed suspension. A freshly prepared solution of l-ascorbic acid (25 mL) was then added drop wise into the above suspension with constant stirring and heated at 90 ºC for 4 h. The obtained black precipitates signify the successful reduction of both metal salts and GO. The excess of ascorbic acid can be eradicated from the product using H_2O_2 solution. The solid product was separated by centrifugation followed by washed with ethanol and deionized water and finally dried in an oven at 65 ^oC.

Catalytic test

In a typical Biginelli reaction experiment, a mixture of 1 mmol of benzaldehyde, 1 mmol of ethyl acetoacetate, 0.8 mmol of urea, 5 mL solvent and 10 mg catalyst were added into a 50 mL round bottom flask and the reaction mixture was kept under vigorous stirring. The reaction progress was screened by TLC. The reaction mixture was filtered; the solvent was evaporated from the

filtrate under reduced pressure to achieve a solid product. However, separation was carried out by column chromatography over silica gel using petroleum ether and ethyl acetate as an eluent. The pure products were characterized by (^{1}H & ^{13}C NMR, FTIR) spectral analysis and compared with reported data as given in Supplementary section, however, melting point (ºC) of products are given in Table 1.

Conflicts of interest

The authors declare no conflict of interest.

Acknowledgements

We express our gratitude to the Head, Applied Chemistry Department, Faculty of Technology & Engineering, The Maharaja Sayajirao University of Baroda, Vadodara, Gujarat, India, for providing the necessary laboratory facilities. The authors would like to present his deep thanks and gratitude to Dr. R. J. Choudhary, Synchrotrons Utilisation Section, Raja Ramanna Centre for Advanced Technology, Indore, India for the help in carrying out work on the Indus-1 synchrotron source.

Keywords: C-C coupling, reduced graphene oxide nanosheet, supported catalysts, ZnO nanoparticles

References

1. C.X. Su, J.F. Mouscadet, C.C. Chiang, H.J. Tsai, L.Y. Hsu, *Chem. Pharm. Bull*., **2006**, 54, 682.
2. R. Chikhale, S. Menghani, R. Babu, R. Bansode, G. Bhargavi, N. Karodia, M. V. Rajasekharan, A. Paradkar, P. Khedekar, *Eur. J. Med. Chem.* **2015**, 96, 30−46.
3. K. L. Dhumaskar, S. N. Meena, S. C. Ghadi, S. G. Tilve, *Bioorg. Med. Chem. Lett*. **2014**, 24, 2897–2899
4. M. Kidwai, S. Saxena, M. K. R. Khan, S. S. Thukral, *Eur. J. Med. Chem.* **2005**, 40, 816–819.
5. J. X. Li, Z. X. Du, L. Y. Xiong, L. L. Fu, W. B. Bo, *J. Solid. State Chem.* **2021**, 293, 121799.
6. J. X. Li, Z. X. Du, Q.Y. Pan, L. L. Zhang, D. L. Liu, *Inorg. Chim. Acta* **2020**, 509, 119677.
7. Y.-J. Liang, G. Feng, X. Zhang, J. X. Li, Y. Jiang, *J. Struct. Chem*., **2021**, 62, 300.
8. Z. Zheng, P. Xu, Y. Jiang, Y. J. Liang, J.-X. Li, *J. Struct. Chem*. **2021**, 62, 292.
9. M. Barbero, S. Cadamuro, S. Dughera, *Green Chem*. **2017**, 19, 1529–1535
10. G. Kour, M. Gupta, S. Paul, V.K. Gupta Rajnikant, *J. Mol. Catal. A: Chem.* **2014**, 392, 260–269.
11. (a) T. Boer; A. Amore; R.V.A. Orru, *Microwaves in Organic Synthesis*, 2nd Edn, Wiley-VCH, Weinheim, **2006**, pp. 788-819; (b) M. Malacria, *Chem. Rev.* **1996**, 96, 289-306.
12. (a) C. D. Graaff; E. Ruijter; R. V. A. Orru, *Chem. Soc. Rev.* **2012**, 41, 3969-4009; (b) M. M. Heravi; S. Asadi; B. M. Lashkariani, *Mol. Divers*. **2013**, 17, 389-407.
13. K. S. Atwal; G. C. Rovnyak; S. D. Kimball; D. M. Floyd; S. Moreland; B. N. Swanson; J. Z. Gougoutas; J. Schwartz; K. M. Smillie; M.F. Malley, *J. Med. Chem.* **1990**, 33, 2629-2635.
14. (a) T. M. Mayer; T. M. Kapoor; S. J. Haggarty; R. W. King; S. L. Schreiber; T. J. Mitchison, *Science* **1999**, 286, 971-974; (b) C. O. Kappe; O. V. Shishkin; G. Uray; P. Verdino, *Tetrahedron* **2000**, 56, 1859-1862.
15. C. O. Kappe, *Acc. Chem. Res.* **2000**, 33, 879-888.
16. L. Heys; C. G. Moore; P. J. Murphy, *Chem. Soc. Rev.* **2000**, 29, 57-67.
17. D. Astruc; F. Chardac, *Chem. Rev.* **2001**, 101, 2991-3024.
18. B. Helms; J. M. J. *Fréchet, Adv. Synth. Catal.* **2006**, 348, 1125-1148.
19. M. Shema-Mizrachi; G. M. Pavan; E. Levin; A. Danani; N. G. Lemcoff, *J. Am. Chem. Soc.* **2011**, 133, 14359-14367.
20. E. L. Margelefsky; R. K. Zeidan; M. E. Davis, *Chem. Soc. Rev.* **2008**, 37, 1118-1126.

21. A. Mondoli; M. Lessi; D. Pini; C. Evangelisti; P. Salvadori, *Adv. Synth. Catal.* **2008**, 350, 375-379.

22. K. Ding; Z. Wang; L. Shi, *Pure Appl. Chem.* **2007**, 79, 1531-1540.

23. Z. Wang; G. Chen; K. Ding, *Chem. Rev.* **2009**, 109, 322-359.

24. L. Marchetti; M. Levine, *ACS Catal.* **2011**, 1, 1090-1118.

25. Z. Zhang; Z. Wang, *J. Org. Chem.* **2006**, 71, 7485-7487.

26. S. B. Kim; P. D. Pike; D. A. Sweigart, *Acc. Chem. Res.* **2013**, 46, 2485-2497.

27. B. M. Choudhary; R. M. Sharma; K. K. Rao, *Tetrahedron* **1992**, 48, 719-726.

28. L. Djakovitch; M. Wagner; C. G. Hartung; M. Beller; K. Kohler, *J. Mol. Catal. A* **2004**, 219, 121-130.

29. L. Yin; J. Liebscher, *Chem. Rev.* **2007**, 107, 133-173.

30. N. Pal; A. Bhaumik, *RSC Adv.* **2015**, 5, 24363-24391.

31. Y. -B. Huang; J. Liang; X. -S. Wang; R. Cao, *Chem. Soc. Rev.* **2017**, 46, 126-157.

32. H. Li; Q. Pan; Y. Ma; X. Guan; M. Xue; Q. Fang; Y. Yan; V. Valtchev; S. Qiu, *J. Am. Chem. Soc.* **2016**, 138, 14783-14788 .

33. H. Wang; C. Wang; Y. Yang; M. Zhao; Y. Wang, *Catal. Sci. Technol.* **2017**, 7, 405-417.

34. H. Li; J. He; A. Riisager; S. Saravanamurugan; B. Song; S. Yang, *ACS Catal.* **2016**, 6, 7722-7727.

35. J. Du; M. Tao; W. Zhang, *ACS Sustain. Chem. Eng.* **2016**, 4, 4296-4304.

36. L. V. Chopda, P. N. Dave, *ChemistrySelect* **2020**, 5, 5552-5572.

37. D. Bhuyan; M. Saikia; L. Saikia, *Catal. Commun.* **2015**, 58, 158-163.

38. X. Huo; J. Liu; B. Wang; H. Zhang; Z. Yang; X. She; P. Xi, *J. Mater. Chem. A* **2013**, 1, 651-656.

39. D. Elhamifar; D. Elhamifar; F. Shojaeipoor, *J. Mol. Catal. A* **2017**, 426, 198-204.

40. Y. Chen; Z. Hu; Y. Chang; H. Wang; Z. Zhang; Y. Yang; H. Wu, *J. Phys. Chem. C* **2011**, 115, 2563-2571.

41. B. Li; H. Cao, *J. Mater. Chem.* **2011**, 21, 3346-3349.

42. K. S. Shin; H. Jo; H. -J. Shin; W. M. Choi; J. -Y. Choi; S. -W. Kim, *J. Mater. Chem.* **2012**, 22, 13032-13038.

43. A. Kumar; D. Saxena; M. Gupta, *Green Chem.* **2013**, 15, 2699-2703.

44. P. Ghosh; A. Das, *J. Org. Chem.* **2013**, 78, 6170-6181.

45. U. Rajesh; J. Wang; S. Prescott; T. Tsuzuki; D. Rawat, *ACS Sustain. Chem. Eng.* **2015**, 3, 2397-2404.

46. Z. Li; H. Zhao; H. Han; Y. Liu; J. Song; W. Huo; W. Chu; Z Sun, *Tetrahedron Lett.* **2017**, 58, 3984-3988.

47. Q. Zhang; C. G. Tian; A. P. Wu; T. Tan; L. Sun; L. Wang; H. Fu, *J. Mater. Chem.* **2012**, 22, 11778-11784.

48. D. Patel; R. Vithalani; C. K. Modi, *New J. Chem.*, **2020**, 44, 2868-2881.

49. R. Vithalani; D. Patel; C. K. Modi; V. Sharma; P. K. Jha, *Appl. Organomet. Chem.* **2020**, 34, e5500.

50. R. Vithalani; D. Patel; C. K. Modi; N. N. Som; P. K. Jha; S. R. Kane, *Diam. Relat. Mater.* **2018**, 90, 154-165.

51. A. Bahuguna; A. Kumar; T. Chhabra; A. Kumar; V. Krishnan, *ACS Appl. Nano Mater.* **2018**, 1, 6711–6723.

52. Y. Zhu; S. Murali; W. Cai; X. Li; J. W. Suk; J. R. Potts; R. S. Ruoff, *Adv. Mater.* **2010**, 22, 3906–3924.

53. S. Mondal; S. Sudhu; S. Bhattacharya; S. K. Saha, *J. Phys. Chem. C* **2015**, 119, 27749-27758.

54. F. Tuinstra; J. L. Koenig, *J. Chem. Phys.* **1970**, 53, 1126-1130.

55. B. Helms; J. M. J. Fréchet, *Adv. Synth. Catal.* **2006**, 348, 1125-1148.

56. S. Yang; X. Feng; S. Ivanovici; K. Muellen, *Angew. Chem. Int. Ed.* **2010**, 49, 8408-8411.

57. K. B. Babitha; J. Jani Matilda; A. P. Mohamed; S. Ananthakumar, *RSC Adv.* **2015**, 5, 50223-50233.

58. D. Bhuyan; M. Saikia; L. Saikia, *Micropor. Mesopor. Mater.* **2018**, 256, 39-48.

59. Z. Ghadamyari; A. Shiri; A. Khojastehnezhad; S. M. Seyedi, *Appl. Organometal Chem.* **2019**, 33, e5091.

60. J. Mondal; T. Sen; A. Bhaumik, *Dalton Trans.* **2012**, 41, 6173-6181.

61. J. Ma; L. Zhong; X. Peng; R. Sun, *Green Chem.* **2016**, 18, 1738-1750.

62. T. K. Pal; D. De; S. Senthilkumar; S. Neogi; P. K. Bharadwaj, *Inorg. Chem.* **2016**, 55, 7835-7842.

63. X. L. Shi; H. Yang; M. Tao; W. Zhang, *RSC Adv.* **2013**, 3, 3939-3945.

64. M. M. Heravi; F. Derikvand; F. F. Bamoharram, *J. Mol. Catal. A* **2005**, 242, 173-175.

65. Z. T. Wang; L. W. Xu; C. G. Xia; H. Q. Wang, *Tetrahedron Lett.* **2004**, 45, 7951-7953.

66. S. Prakash, N. Elavarasan, A. Venkatesan, K. Subashini, M. Sowndharya, V. Sujatha, *J. Adv. Powder Technol.* **2018,** 29, 3315-3326.

67. R. Vithalani; D. Patel; C. K. Modi; P. K. Jha; H. Srivastava; S. R. Kane, *Graphene Technol.* **2020**, 5, 83-101.

10.1002/ejic.202100368

Table of Contents

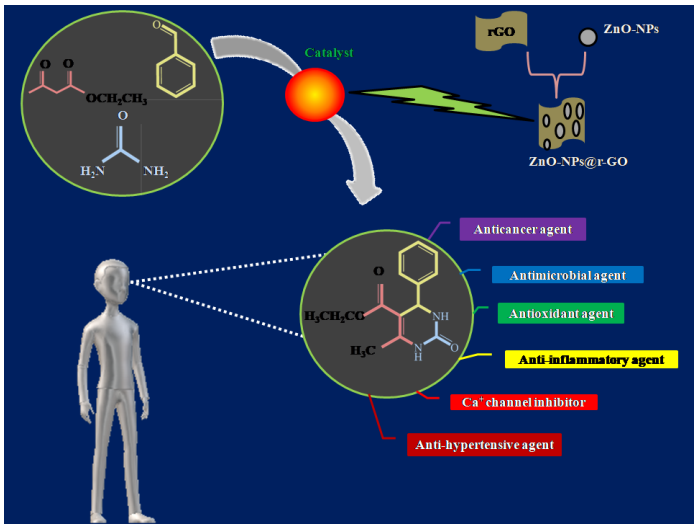

ZnO nanoparticles adorned on reduced graphene oxide nanosheet (ZnO-NPs@r-GO) have shown admirable catalytic activity for multicomponent one-pot A^3-coupling reaction under mild reaction conditions to give preferred 3,4-dihydropyrimidinones products in good to venerable yields.